Interannual variability and trend of CH4 lifetime as a measure for OH changes in the 1979-1993 time period

Dentener, Frank; Peters, Wouter; Krol, Maarten; van Weele, Michiel; Bergamaschi, Peter; Lelieveld, Jos

Published in:
Journal of Geophysical Research

DOI:
10.1029/2002JD002916

Publication date:
2003

Interannual variability and trend of CH_4 lifetime as a measure for OH changes in the 1979–1993 time period

Frank Dentener,[1] Wouter Peters,[2] Maarten Krol,[2] Michiel van Weele,[3] Peter Bergamaschi,[1] and Jos Lelieveld[4]

Received 6 September 2002; revised 31 March 2003; accepted 1 May 2003; published 2 August 2003.

[1] The interannual variability and trend in the CH_4 lifetime, as a measure for global mean OH concentration, have been analyzed systematically with three-dimensional (3-D) chemistry-transport model simulations. It is shown that the global mean OH concentration is highly variable from year to year due to changes in meteorology, changes in tropospheric UV radiation intensities, and changes in chemical concentrations owing to variable emissions of photochemical precursor gases (CH_4-CO-NMVOC-NO_x). The meteorological variability is taken into account with the ECMWF-ERA15 1979–1993 reanalysis. Satellite observations provide the observed changes in the stratospheric ozone concentrations. Emission inventories are used to account for trends in anthropogenic emissions and their patterns. For the period 1979–1993, our simulations indicate a decrease of the calculated global tropospheric methane lifetime from 9.2 to 8.9 years, corresponding to a positive OH trend of $0.24 \pm 0.06\%$ yr^{-1}. The modeled trend is mostly determined by changes in the tropical tropospheric water vapor content, while the changes in photolysis rates and in surface emissions of reactive trace gases compensate in their effect on the calculated OH trend over the analyzed time period. *INDEX TERMS:* 0322 Atmospheric Composition and Structure: Constituent sources and sinks; 0325 Atmospheric Composition and Structure: Evolution of the atmosphere; 0365 Atmospheric Composition and Structure: Troposphere—composition and chemistry; *KEYWORDS:* OH radical, hydroxyl, CH_4 lifetime, variability, trend, global

Citation: Dentener, F., W. Peters, M. Krol, M. van Weele, P. Bergamaschi, and J. Lelieveld, Interannual variability and trend of CH_4 lifetime as a measure for OH changes in the 1979–1993 time period, *J. Geophys. Res.*, *108*(D15), 4442, doi:10.1029/2002JD002916, 2003.

1. Introduction

[2] The main oxidant removing atmospheric trace gases from the atmosphere is the hydroxyl (OH) radical. Model simulations suggest that global OH changed between +7% [*Berntsen et al.*, 1997; *Martinerie et al.*, 1995] and −9% to −15% [*Wang and Jacob*, 1998; *Lelieveld et al.*, 2002] during the last century. Further decreases of 10% to 20% are expected to happen in the 21st century, as indicated by *Prather et al.* [2001]. At present the possibilities to determine large-scale OH concentrations and the associated trends are limited to the use of methyl-chloroform (MCF) observations from the ALE/GAGE/AGAGE and NOAA/CMDL networks, combined with a priori knowledge on emissions, and utilizing atmospheric transport-chemistry model inversions. Unfortunately, the results and their interpretation of different studies are somewhat ambiguous. *Prinn et al.* [1995] and *Prinn and Huang* [2001] used MCF observations to derive an OH trend of $0.0\% \pm 0.2\%$ yr^{-1} for the period 1978–1993. In contrast, using the same observational data-set, but a different statistical analysis technique and assumptions on initial pre-1978 conditions, *Krol et al.* [1998, 2001] derive a positive OH trend of $0.46 \pm 0.6\%$ yr^{-1} for this period. In a recent study, *Prinn et al.* [2001] derive a strong upward trend of OH by $15 \pm 22\%$ for the period 1979–1989 ($1.4 \pm 2.1\%$ yr^{-1}), followed by a drastic decrease by 25% (with probably a similar uncertainty range) in the period 1990–2000 (−2.3% yr^{-1}). Similar trends were computed by *Krol and Lelieveld* [2003], who, however, also discuss major problems with the use of methyl-chloroform data to derive OH, possibly due to the presence of unexpected ongoing emissions in Europe [*Krol et al.*, 2003]. Given these uncertainties, it is important to further analyze these computed trends and try to understand the possible causes.

[3] In this paper we examine the interannual variability of the CH_4 lifetime as a measure for the change in the global mean OH concentration. Specifically, we want to untangle the possible causes for interannual OH variability: interannual changes in the meteorology, changes in stratospheric ozone concentrations, and changes in emissions and concentrations of CH_4, CO, NMVOC (non-methane-volatile

[1]Institute for Environment and Sustainability, Joint Research Centre, Ispra, Italy.
[2]Instituut voor Marien en Atmosferisch Onderzoek Utrecht, Utrecht University, Utrecht, Netherlands.
[3]Department of Applied Physics, Eindhoven University of Technology, Eindhoven, Netherlands.
[4]Max-Planck-Institute for Chemistry, Mainz, Germany.

0148-0227/03/2002JD002916

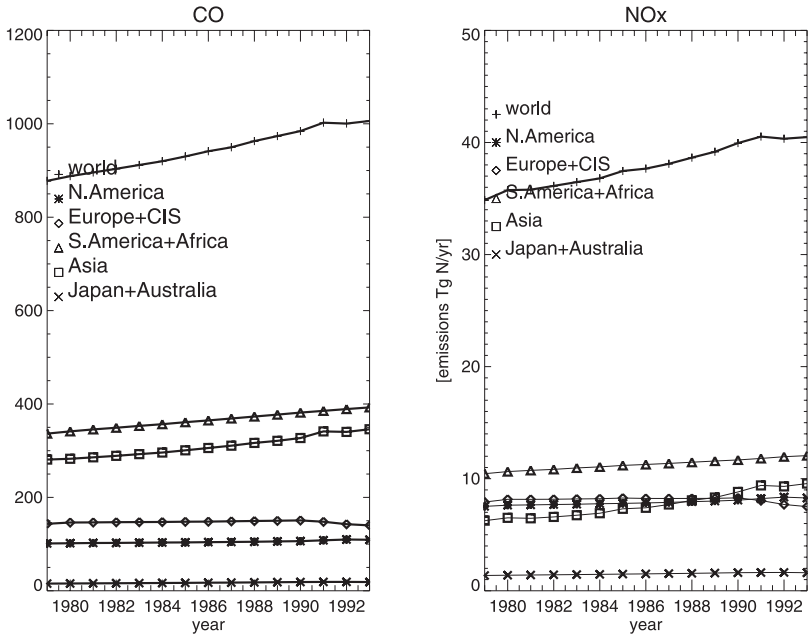

Figure 1. Temporal development of CO [Tg CO yr^{-1}] and NO_x [Tg N yr^{-1}]. Note that the vegetation and ocean CO emissions are not included in this figure, and would add an additional 115 Tg CO yr^{-1}. See color version of this figure in the HTML.

organic carbons) and NO_x. We perform a systematic analysis using eleven long-term model simulations for the period 1979–1993. We use the global chemistry-transport model TM3 (Tracer Model version 3) with meteorological data from the ECMWF (European Centre for Medium Range Weather Forecast) reanalysis for the years 1979–1993 (ERA15) [*Gibson et al.*, 1997]. Satellite observations of total ozone columns are from the Total Ozone Mapping Spectrometer (TOMS) [*McPeters*, 1996] and we use a recent database of global anthropogenic emissions and their trends [*van Aardenne et al.*, 2001].

[4] In section 2 we briefly describe our model, in section 3 we present the results, and we end in section 4 with a detailed discussion of our results and give our main conclusions.

2. Method

2.1. Model Description

[5] The global chemistry-transport model TM3 [*Dentener et al.*, 2003, and references therein] has been used in this study at a spatial resolution of 10° longitude and 7.5° latitude with 19 vertical layers. The model uses six-hourly ERA15 meteorological fields [*Gibson et al.*, 1997]. These fields include global distributions for horizontal wind, surface pressure, temperature, humidity, cloud liquid water content, cloud ice water content, cloud cover, large-scale and convective precipitation. We showed before that the model realistically simulates radon 222 [*Dentener et al.*, 1999], tropospheric ozone [*Houweling et al.*, 1998; *Lelieveld and Dentener*, 2000; *Peters et al.*, 2001], and methane [*Houweling et al.*, 2000; *Dentener et al.*, 2003]. The model has been further used for numerous other studies. Some of the above mentioned evaluation studies have been performed using a model version with a higher horizontal resolution (5° × 3.75°). However, since in both cases the model uses interpolated high-resolution meteorological input data, large-scale patterns of water vapor, temperature, and circulation, and their possible trends, are well represented even in the coarsest resolution. In the present study the chemical scheme described by *Houweling et al.* [1998] and *Dentener et al.* [2003] has been used.

[6] Yearly anthropogenic emissions of the reactive trace gases NO_x, CO, and NMVOC are taken from the emission database developed by *van Aardenne et al.* [2001], which is based on the widely used EDGAR2.0 emission database [*Olivier et al.*, 1999], and describes the development of emissions during the period 1890–1990. We used the base years 1970, 1980, 1985, and 1990, and linearly interpolated the emissions for the years 1979–1990. Emissions for the period 1991–1993 are obtained by extrapolation of the 1990 data using the geographically distributed CO_2 emission statistics from *Marland et al.* [2000]. Natural emissions of NO_x (soils and lightning), CO (soils and vegetation), and NMVOC (vegetation) are as described by *Houweling et al.* [1998] and assumed to be constant during the simulation period, with the exception of NO_x production from lightning discharges which is coupled to model convection and shows an interannual variability of about 0.5 Tg N yr^{-1} or 10%.

[7] We show the development of the global and regional annual NO_x and CO emissions for the period 1979–1993 in Figure 1 and in Table 1. The calculated yearly global NO_x emissions increase by about 6 Tg N (or 17% of the total emissions in 1979) in the period 1979–1993, CO by about 55 Tg CO or 13%, and NMVOC by 37 Tg C or 3%. The increases are entirely due to increased economic activity in Asia, Africa and S. America, whereas the emissions in North America and Europe have leveled off or declined.

[8] For methane a somewhat different approach was followed, as described more extensively by *Dentener et al.* [2003]. Following *Houweling et al.* [2000], we firstly apply annually constant anthropogenic and natural emissions, valid for the 1980s amounting to 531 Tg CH_4 yr^{-1}.

Table 1. Annual Natural, Anthropogenic, and Total NO_x CH_4, CO, and NMVOC Emissions[a]

Year	NO_x[b], Tg N yr^{-1}	CH_4[c], Tg CH_4 yr^{-1}	CO[d], Tg CO yr^{-1}	NMVOC[e], Tg C yr^{-1}
1979	7.6-26.7-34.3	159.5-372.0-495.9	115.1-877.5-992.6	320.4-121.3-441.7
1980	7.4-27.6-35.0	159.5-372.0-494.9	115.1-889.6-1004.6	320.4-124.2-444.6
1981	7.4-27.7-35.1	159.5-372.0-507.6	115.1-895.4-1010.5	320.4-125.4-445.8
1982	7.4-28.0-35.6	159.5-372.0-507.2	115.1-903.3-1018.4	320.4-126.8-447.2
1983	7.6-28.4-36.0	159.5-372.0-521.8	115.1-911.4-1026.5	320.4-128.3-448.7
1984	7.6-28.8-36.4	159.5-372.0-520.2	115.1-922.0-1037.1	320.4-130.0-450.4
1985	7.3-29.4-36.7	159.5-372.0-524.3	115.1-929.6-1044.7	320.4-131.3-451.7
1986	7.3-29.7-37.0	159.5-372.0-518.7	115.1-939.7-1054.8	320.4-134.4-454.8
1987	7.4-30.1-37.5	159.5-372.0-530.2	115.1-950.0-1065.1	320.4-137.6-458.0
1988	7.6-30.8-38.4	159.5-372.0-537.9	115.1-963.5-1078.6	320.4-141.5-461.9
1989	7.7-31.2-38.9	159.5-372.0-528.8	115.1-972.4-1087.5	320.4-144.8-465.2
1990	7.6-32.1-39.5	159.5-372.0-547.2	115.1-983.6-1098.7	320.4-148.3-468.7
1991	7.6-32.6-40.2	159.5-372.0-540.9	115.1-1001.3-1116.4	320.4-156.6-477.0
1992	7.3-32.6-39.9	159.5-372.0-538.1	115.1-1002.7-1117.8	320.4-155.4-475.8
1993	7.6-32.6-40.2	159.5-372.0-524.4	115.1-1006.3-1121.4	320.4-157.7-478.1

[a]Emissions from high-latitude wildfires were not included in this simulation.
[b]Natural NO_x emissions from lightning and stratospheric influx of NO_y, soil emissions are included in the anthropogenic category.
[c]Natural emissions include a soil oxidation sink of −30 Tg CH_4 yr^{-1}. The total reflects the emissions effectively entering the calculations, and include an anthropogenic trend, as well as natural variability. See text and *Dentener et al.* [2003].
[d]Natural CO emissions from soils and vegetation.
[e]Natural NMVOC emissions from isoprene.

We then adjusted the surface methane mixing ratios using a nudging technique [*Dentener et al.*, 2003], and surface observations from the NOAA network [*Dlugokencky et al.*, 1998]. This effectively adjusts emissions to match the observations. In the period 1979–1993 global methane mixing ratios increased by about 11% from 1557 ppbv to 1730 ppbv. The emission trend calculated from mass balance considerations favorably compared with the independent estimate of anthropogenic emissions trends of 2.7 Tg CH_4 yr^{-1} presented by *van Aardenne et al.* [2001]. The remaining signal was attributed to interannual variability in CH_4 emissions in the order of 8 Tg CH_4 yr^{-1}. To our knowledge natural CH_4 emissions have a variability of at least this order of magnitude. The emissions effectively entering the calculations are listed in Table 1. The implications of this nudging procedure for the calculated trends are further discussed in section 4.

[9] Stratospheric boundary conditions for ozone were applied by relaxation of stratospheric ozone at levels above 50 hPa toward the zonal and monthly mean ozone column measurements by the Total Ozone Mapping Spectrometer (TOMS) [*McPeters*, 1996]. The vertical distribution of ozone was taken from a climatology representative for the 1980s [*Fortuin and Kelder*, 1998]. The ozone column above 10 hPa is prescribed using the same climatology. Below 50 hPa, other than by chemical processes, there were no further constraints, and the 3-D ozone variability in the rest of the stratosphere is maintained by simulated transport. Since TOMS measurements are not available for a large part of the year 1993, we applied the 1992 ozone columns also for the year 1993. The validation of stratosphere-troposphere exchange in the period 1979–1993 was limited by a lack of measurement data. Therefore *Lelieveld and Dentener* [2000] used a number of Northern Hemispheric ozone soundings with proven reliability, to show that the ozone in the vicinity of the tropopause (200 hPa) was realistically reproduced, meaning that in the free troposphere monthly averaged ozone concentrations were generally within 5–10 pbbv, and a very realistic representation of the seasonal cycle. However, at 200 hPa level, the model did not reproduce some of the highest peaks associated with stratospheric intrusions in the troposphere. The stratosphere-troposphere exchange flux of 565 Tg O_3 yr^{-1} is fairly consistent with the current view on the magnitude of this flux [*Prather et al.*, 2001]. We showed [*Lelieveld and Dentener*, 2000] that this technique results also in realistic values for atmospheric and tropospheric ozone columns of about 20 DU, in agreement with a host of other models, and observations. Both measured and modeled ozone trends in the background troposphere differed at various locations, but were generally small. Unfortunately, we had only few long-term tropical measurements of O_3 to our disposal. The two background tropical stations, Mauna Loa and Samoa, showed a very favorable agreement of measured and modeled ozone, with deviations of long-term monthly averaged O_3 smaller than 3 pbbv. The resulting effect of ozone abundance and variability on photolysis frequencies and hence on OH are calculated with the scheme by *Landgraf and Crutzen* [1998], including the effects of clouds, surface albedo and the overhead ozone column following *Krol and Van Weele* [1997].

2.2. Simulations

[10] In order to analyze the changes in OH and CH_4 lifetimes, we performed eleven simulations S1–S11 (Table 2) covering the ERA15 period (1979–1993). All simulations used a spin-up time of 2 years. In the base simulation S1 we apply the full interannual variations and trends of model boundary conditions, i.e., we use meteorology, emissions and stratospheric ozone of the corresponding years.

[11] This simulation has been used in previous analyses of the ozone budget as described by *Lelieveld and Dentener* [2000] and [*Peters et al.*, 2001]. Both studies showed that ozone was realistically represented at various locations over the globe, and a clear correlation of tropical [19S–19N] ozone with the El Niño–Southern Oscillation (ENSO) index was found, in good agreement with an earlier analysis of satellite observations [*Ziemke and Chandra*, 1999]. Additionally, *Dentener et al.* [2003] showed that S1 produces a consistent picture of the methane budget, meaning

Table 2. List of Simulations

Simulations	Description	Meteorology	Emissions	CH_4	Stratospheric O_3
S1	full simulation	1979–1993	1979–1993	1979–1993	1979–1992
S2	meteorology	1979–1993	1993	1993	1992
S3	all emissions + strat. O_3	1993	1979–1993	1979–1993	1979–1992
S4	stratospheric O_3	1993	1993	1993	1979–1992
S5	CO, NO_x, NMVOC emissions + CH_4 increases	1993	1979–1993	1979–1993	1992
S6	CH_4 increases	1993	1993	1979–1993	1992
S7	CO emissions	1993	1979–1993	1993	1992
S8	NO_x emissions	1993	1979–1993	1993	1992
S9	NMVOC emissions	1993	1979–1993	1993	1992
S10[a]	humidity/temperature	1993	1993	1993	1992
S11[b]	wet removal + clouds	1993	1993	1993	1992

[a]S10 includes varying humidity and temperature fields for the years 1979–1993.
[b]S11 included varying cloud and precipitation fields for the years 1979–1993.

that the calculated CH_4 emission trend compared very well with atmospheric observations and an independent emission estimate by *van Aardenne et al.* [2001]; see also section 2.1.

[12] In S2 we applied the meteorology for the years 1979–1993, while the reactive precursor gas emissions, the nudged CH_4 surface concentrations, and stratospheric ozone columns were kept representative for the year 1993. In contrast, in simulation S3 we used one repeated meteorological year (1993), while the emissions and stratospheric ozone varied from year-to-year. Simulation S4 combines 1993 meteorology and emissions with a year-to-year variability of stratospheric ozone concentrations alone. In simulation S5, surface emissions of CO, NMVOC, NO_x and nudged concentrations of CH_4 were varied, while meteorology and stratospheric ozone were specified for 1993, and 1992 respectively. In S6 we varied only the methane surface concentration constraints while all other conditions (emissions, meteorology) remained representative for 1993. This simulation isolates the effect of changing methane abundances on the CH_4 lifetime. In S7, S8 and S9, only the CO, NO_x and NMVOC emissions are varied.

[13] Finally, simulations S10 and S11 isolate the effects of the variability of moisture, temperature and the combined effect of wet scavenging and cloud amounts for comparison with simulation S2. For this purpose in S10 only the humidity and temperature fields were changed on an annual basis, whereas in S11 the cloud- and precipitation fields were varied for the years 1979–1993. S11 thus analyses the effects of changing wet deposition as well as changes in photolysis rates due to cloud cover, which unfortunately could not be separated. All other conditions in S10 and S11 were representative for 1993.

[14] For post-analysis we stored the monthly averaged three-dimensional OH fields from the eleven simulations to perform calculations of CH_4 lifetimes. Deviations resulting from the use of the monthly averaged OH fields, as compared to the on-line photo-chemistry calculations were evaluated to be small. Note that, owing to the influence of the preceding years, small deviations between the various simulations of 1993 may occur. However, they are not important for the results presented in this work.

3. Results

[15] Annual variations of transport patterns, changing emissions and changes in chemical boundary conditions lead to changing OH and CH_4 concentrations, which together determine the CH_4 lifetime. Following the recommendations of [*Lawrence et al.*, 2001] we analyze the changes in global mean OH weighted to the reaction with methane (i.e., the chemical methane lifetime). The tropospheric chemical lifetimes of CH_4 are calculated as the quotient of the annual average tropospheric burden and the destruction rates of CH_4 by tropospheric OH. We compute the global tropospheric averages and for four zonal regions (45N–90N, 0–45N, 0–45S, and 45S–90S). In our analysis we use a fixed altitude of 100 hPa to define the tropopause.

[16] In Figure 2 we show the tropospheric lifetimes of methane calculated for the reference simulation (S1) as well as the sensitivity simulations S2 and S3. To further examine the chemical signal, we show in Figure 3 the results of simulations S3, S4, and S5. Figure 4 further evaluates the meteorology-only simulation and displays S2, S10, and S11. The results are summarized in Table 3.

3.1. Methane Lifetimes and Global Mean OH

[17] Averaged over the period 1979–1993 the annual and global average tropospheric CH_4 chemical lifetime for base simulation S1 is about 9.0 years, which can be compared with a range of 6.5–9.8 year, evaluated by *Prather et al.* [2001]. The calculated lifetimes of base simulation S1 averaged for 1979–1993 are about 28 and 55 years in the NH and SH high latitude regions, respectively, and 6.4 years and 7.5 years for the 45N–0 and 0–45S latitude regions. As noted by *Lawrence et al.* [2001] comparisons of global mean OH is somewhat hampered by differences in averaging methods. This global lifetime of 9.0 ± 0.13 years (see Table 3) years corresponds to a global mass-averaged OH concentration of about 1.00 10^6 molecules cm^{-3}. Using the climatological tropopause recommended by *Lawrence et al.* [2001] the calculated chemical lifetime of CH_4 would be about 6% lower (8.5 years), corresponding to a mass-weighted global average OH concentration of 1.06 10^6 molecules cm^{-3}. Note however, that in this work we analyze the changes of OH in terms of methane chemical lifetimes, thus weighted to the reaction of OH and CH_4.

3.2. Trends and Variability of S1, S2, and S3

[18] For the period 1979–1993, simulation S1 indicates a statistically significant decrease of methane lifetimes in all four regions by 0.21% to −0.37% yr^{-1} (Table 3).

[19] Globally, the calculated tropospheric methane lifetime decreases from 9.2 to 8.9 years (−0.24 ± 0.06% yr^{-1}) over 15 years. The uncertainty interval corresponds to the

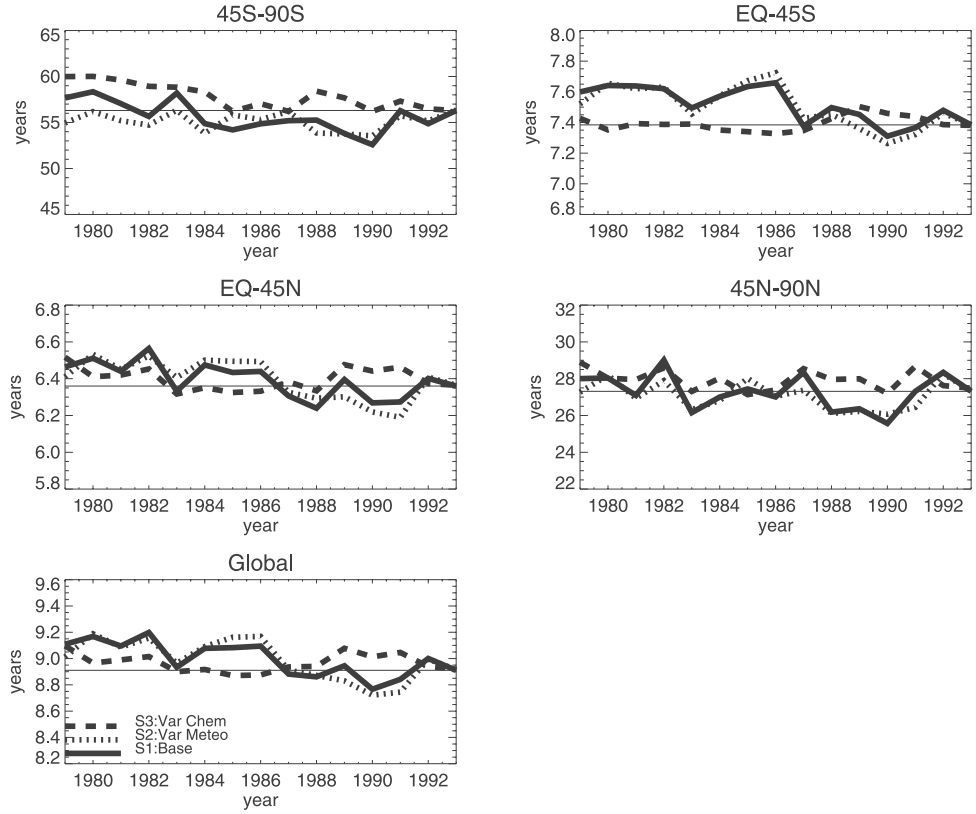

Figure 2. Methane lifetimes [years] for simulations S1 (solid line), S2 (short-dashed line) and S3 (long-dashed line). Results are given for four regional compartments as well as for the whole troposphere. Horizontal line indicates lifetime of 1993. Note that nonlinear effects are present in the simulations. See color version of this figure in the HTML.

±1 σ standard deviation of the regression analysis. Therefore it does not evaluate the uncertainty in the model representation of transport, chemistry and emissions, which may further contribute to the uncertainty of the OH trend and variability.

[20] The global lifetime of methane is strongly determined by the (sub)tropical regions, since high OH concentrations and temperatures favor methane destruction. The simulated global decrease of CH_4 lifetimes (and increase of OH) is therefore most strongly determined by meteorological factors (S2). However, Figure 2 together with Table 3 clearly shows that the calculated trend and variability in S1 is also a complicated combination of meteorological variability (S2) and chemical concentration changes due to variable emissions and stratospheric O_3 (S3). In the high latitude Southern Hemisphere most of the trend is caused by the chemical changes, while most of the trend (-0.27 ± 0.06) in the region 45S-EQ is controlled by meteorology. The trend signal (-0.21 ± 0.07) in the region 45N-EQ is a mixture of meteorology (-0.23 ± 0.09) and chemical changes (-0.03 ± 0.06), whereas in the 45N–90N region the lifetimes do not show a significant trend (-0.21 ± 0.21). Note here that due to non-linear effects of chemistry and transport, we do not expect the combined trend signal of S2 and S3 to exactly match that of S1.

[21] In Table 4 we investigate the likelihood that the signal of one simulation can be explained by two other simulations. Multiple-linear regression analysis on simulations S1-S2-S3 shows that roughly equal contributions of S2 (55%) and S3 (45%) can explain the global interannual variability for S1 with a high probability (F = 556, χ^2 = 0.99). Also in the subhemispheric compartments the variability of τ_{CH4} can be well explained by equal contributions of simulations S2 and S3. Table 3 also shows that the most of the variability of methane lifetime over the 15 year period can be explained by meteorology. The global variability of τ is about 0.15 year for S2, corresponding to 1.6%.

[22] In section 3.3, we will investigate how meteorological variability affects local OH and CH_4 chemistry. In section 3.4 we evaluate influence of the chemical boundary conditions.

3.3. How the Meteorological Variability Influences τ_{CH4}: Simulations S2, S10, and S11

[23] The interannual variability of τ_{CH4} is caused by either the variability of OH, or the rate constant k_{CH4+OH}. In this section we examine simulations S2, S10 and S11, where the 1993 methane surface layer concentrations were used for the entire period 1979–1993. Therefore variations in methane concentrations do not influence the calculated interannual variability of the CH_4 lifetime. Further, the influence of the temperature on the reaction constant of k_{CH4+OH} is of the order of 2% K^{-1} (between 273 K–300 K). Integrated large-scale average interannual temperature variations in the four atmospheric compartments are of the order of 0.3 K. Therefore we do not expect a strong direct effect of large-scale temperature variations on τ_{CH4}. This leaves the variability of OH as the single most

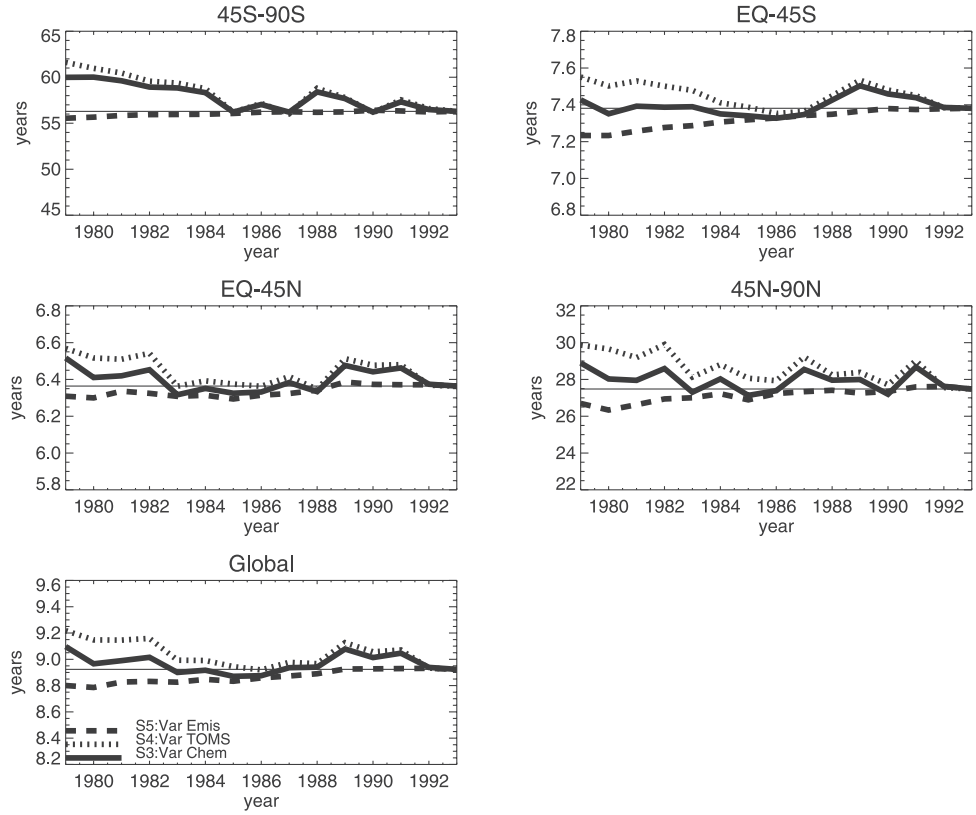

Figure 3. Methane lifetimes [years] for simulations S3 (solid line), S4 (short-dashed line), S5(long-dashed line). Results are given for four regional compartments as well as for the whole troposphere. Horizontal line indicates lifetime of 1993. Note that nonlinear effects are present in the simulations. See color version of this figure in the HTML.

important factor to explain the interannual variability of τ_{CH4} in S2, S10 and S11.

[24] The interannual variability of OH can be caused by variation of the sinks of OH and its primary sources, integrated over a year and per region.

[25] To explain variability in the primary source of OH, the following reaction chain needs to be considered:

$$O_3 \rightarrow O(^1D) + O_2 \tag{1}$$

$$O(^1D) + M(+O_2) \rightarrow O_3 + M \tag{2}$$

$$O(^1D) + H_2O \rightarrow 2OH \tag{3}$$

[26] The production rate of OH P_{OH} [mol region^{-1} year^{-1}] can be obtained by integrating over time and space as given in equation 4:

$$P_{OH} = \int k_{O(^1D)+H_2O}[O(^1D)][H_2O]\delta t \tag{4}$$

[27] Thus variations in moisture, photolysis rates, and ozone abundance can underlie variations in primary OH production. Variations in photolysis rates are strongly controlled by the actinic fluxes and thus the stratospheric ozone concentrations. Ozone variability in the troposphere is governed by the influx of ozone from the stratosphere across the tropopause, as well as variation of in-situ production in the troposphere. Water vapor variations are introduced by meteorological variability as represented in the ECMWF reanalysis.

[28] A major secondary source of OH in the troposphere is the recycling of HO_2 mainly by the reaction with NO and O_3 [*Lelieveld et al.*, 2002; *Derwent*, 1996]. However, variations of this secondary source are not expected to be important for simulation S2.

[29] The chemical sinks are given by the generic reaction 5, which represents all relevant OH sink reactions.

$$RH + OH(+O_2) \rightarrow RO_2 + H_2O \tag{5}$$

[30] The amount of OH consumed in a year and a certain domain S_{OH} [mol region^{-1} year^{-1}] is obtained by adding and integrating all OH sinks as given by equation 6:

$$S_{OH} = \int (k_{CO+OH}[CO] + k_{CH_4+OH}[CH_4] + k_{OH+Isoprene}[Isoprene] + \ldots)\delta t \tag{6}$$

[31] S_{OH} varies from year-to-year, e.g, due to variability of transport processes, and hence concentrations of, e.g., CO, CH_4 etc. Convective variability may transport variable amounts of CO from the boundary layer in the free troposphere, where less OH is available and temperatures

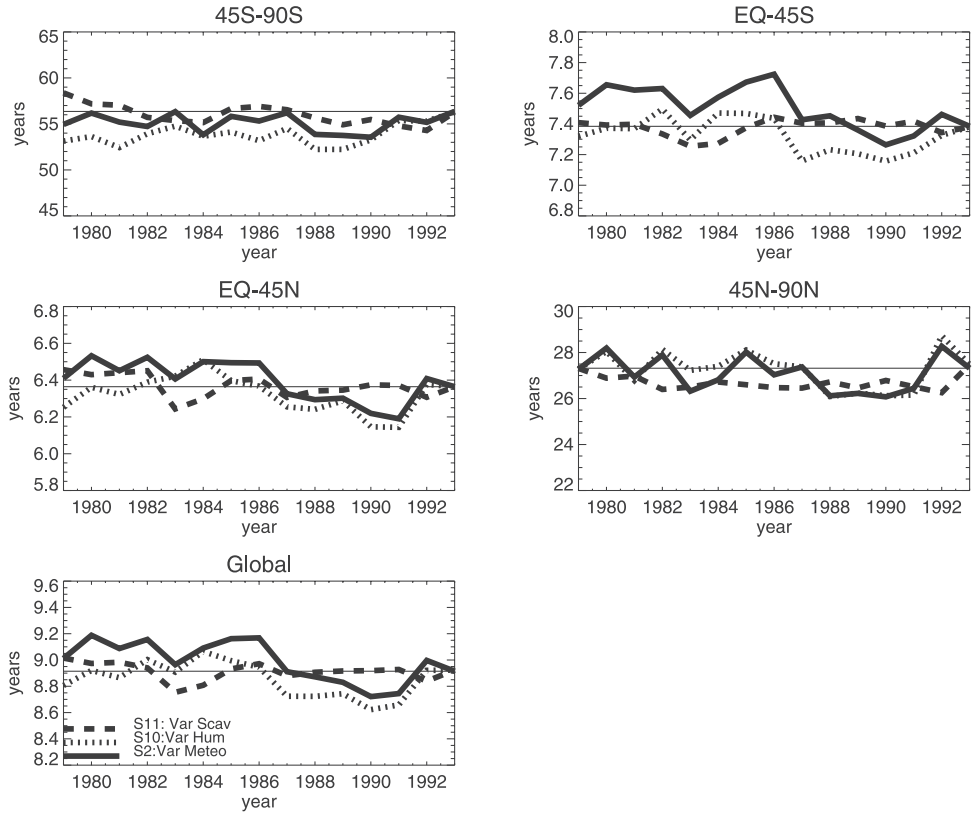

Figure 4. Methane lifetimes [years] for simulations S2 (solid line), S10 (short-dashed line), and S11 (long-dashed line). Results are given for four regional compartments as well as for the whole troposphere. Horizontal line indicates lifetime of 1993. Note that nonlinear effects are present in the simulations. See color version of this figure in the HTML.

are lower. At the same time the transport efficiency of these gases can also change due to the chemical feed-back of changing OH concentrations. Also physical removal of radical precursor gases such as H_2O_2 (e.g. wet scavenging) is subject to interannual variability and can therefore influence the effective radical sink. The effective OH radical loss rate L_{OH} [year^{-1}] is calculated according to equation 7:

$$L_{OH} = S_{OH} / \int [OH] \qquad (7)$$

[32] In Table 5 we show the correlation coefficients of τ_{CH4} with P_{OH} and L_{OH}. P_{OH} highly correlates (r = −0.86 to r = −0.96) with the methane lifetime in sensitivity study S2. This simulation thus includes the effect on P_{OH} of changing humidity patterns, as well as changing ozone in the troposphere. The high correlation is mostly due to water vapor variations as we show in Figure 4. The correlation between large-scale integrated H_2O and τ_{CH4} is also high, except in the region 45S–90S. Also, if we compare the time series of τ_{CH4} of simulations S2 and S10 we find correlation coefficients of r = 0.8 to r = 0.9 in the different regions, which

Table 3. Trend ± Uncertainty of Modeled Trend of Methane Lifetimes for the Period 1979–1993[a]

Simulation	90N–45N	45N–EQ	EQ–45S	45S–90S	Global
S1	−0.21 ± 0.21	−0.21 ± 0.07	−0.27 ± 0.06	−0.37 ± 0.15	−0.24 ± 0.06
S2	−0.15 ± 0.17	−0.23 ± 0.08	−0.26 ± 0.08	−0.04 ± 0.11	−0.23 ± 0.08
S3	−0.14 ± 0.12	−0.03 ± 0.06	0.04 ± 0.04	−0.45 ± 0.09	−0.02 ± 0.05
S4	−0.48 ± 0.12	−0.13 ± 0.07	−0.10 ± 0.05	−0.59 ± 0.11	−0.15 ± 0.05
S5	0.28 ± 0.04	0.08 ± 0.02	0.16 ± 0.01	0.09 ± 0.01	0.12 ± 0.01
S6	0.08 ± 0.01	0.19 ± 0.01	0.25 ± 0.01	0.23 ± 0.01	0.21 ± 0.01
S7	0.09 ± 0.01	0.15 ± 0.00	0.11 ± 0.01	0.17 ± 0.04	0.13 ± 0.01
S8	−0.31 ± 0.04	−0.57 ± 0.02	−0.26 ± 0.02	−0.20 ± 0.06	−0.41 ± 0.02
S9	0.21 ± 0.03	0.22 ± 0.02	0.07 ± 0.01	0.10 ± 0.05	0.15 ± 0.01
S10	−0.16 ± 0.18	−0.12 ± 0.09	−0.15 ± 0.09	0.23 ± 0.12	−0.13 ± 0.09
S11	−0.05 ± 0.08	−0.10 ± 0.05	0.03 ± 0.04	−0.28 ± 0.09	−0.05 ± 0.05
τS1[b]	27.3 ± 0.95	6.4 ± 0.10	7.5 ± 0.11	55.7 ± 1.61	9.0 ± 0.13
τS2[b]	25.1 ± 0.96	6.3 ± 0.10	7.5 ± 0.14	54.3 ± 1.15	8.8 ± 0.15

[a]The real uncertainty of trend will depend on accuracy of model and missing processes. See section 4. Negative CH_4 lifetime trends correspond to positive OH trends. Positive CH_4 lifetime trends correspond to negative OH trends. Values are % year^{-1}.
[b]Average methane lifetime and standard deviation [year] for the period 1979–1993.

Table 4. Results of Multiple Linear Regression Analysis on S1-S2-S3 and S3-S4-S5[a]

Simulations	Parameters	90N–45N	45N–EQ	EQ–45S	45S–90S	Global
S1-S2-S3	A-B	0.55-0.45	0.55-0.45	0.53-0.47	0.55-0.45	0.56-0.44
S1-S2-S3	F-χ^2	111-0.99	168-0.98	232-0.98	83-0.98	556-0.99
S3-S4-S5	A-B	0.47-0.53	0.53-0.47	0.49-0.51	0.58-0.42	0.49-0.51
S3-S4-S5	F-χ^2	77-0.96	81-0.97	149-0.98	702-1.00	99-0.97

[a]A and B values represent the normalized regression coefficients corresponding to S2(S4) and S3(S5), i.e., the relative contribution of S2(S4) and S3(S5) to explain the signal of S1(S3). F and χ^2 are statistical values for the goodness of the regression. χ^2 close to 1 indicates a good fit of the regression, whereas values of F > 3 correspond to a high significance of the fit.

again indicates that water vapor variability dominates the variability of τ_{CH4}. Indeed, if we correct P_{OH} for the variability of O_3 and H_2O (Table 5), thus eliminating their respective influences, we find only in the Southern Hemisphere a dependency of τ_{CH4} on O_3, whereas in the other regions the τ_{CH4} variability depends mostly on H_2O. This is also indicated by the low correlation coefficient of P_{OH}/H_2O. A similar analysis of τ_{CH4} with large scale temperatures variations also showed high correlations, since in the ECMWF meteorological data moisture and temperature variations are closely linked. We conclude that the high correlations of τ_{CH4} and P_{OH} in S2 is largely controlled by water vapor variability.

[33] The interannual variability in OH loss rates (L_{OH}) appears to be dominated by variability in transport of reactants, where especially CO is playing an important role. In the Southern Hemisphere no correlation is found between L_{OH} and τ_{CH4}, whereas in the compartment 45N-EQ a correlation og r = 0.70 is found. A larger variability of OH due to sink reactions can be expected in the Northern Hemisphere than in the Southern Hemisphere, since OH is influenced more strongly by shorter lived trace gases in the Northern Hemisphere. The variability in wet removal of soluble radical precursor gases is not responsible for the variability found in simulation S2 (Figure 4), as the CH_4 lifetime calculated for S11 and S2 correlate only very weakly (r = 0.13).

[34] Thus most of the variability of τ_{CH4} is determined by P_{OH}, whereas in the NH L_{OH} is, less strongly, also influencing τ_{CH4}.

3.4. How Changes in Chemical Boundary Conditions Affect τ_{CH4}: Simulations S3–S9

[35] In this section we focus on the sensitivity study S3 and the individual contributions of the prescribed stratospheric ozone concentration changes (S4), changing concentrations of methane alone (S6), CO emissions (S7), NO_x emissions (S8) and NMVOC emissions (S9) and including the combined effect of the emissions of all precursor gases (NO_x, NMVOC, CO, CH_4) (S5). Figure 3 shows the opposing effects of S4 and S5 on the CH_4 lifetime. In the high latitude regions S4 shows negative CH_4 lifetime trends of -0.48 ± 0.12 (90N–45N) and -0.59 ± 0.11 (45S–90S) % yr^{-1}. In these regions increased UV radiation fluxes (due to decreasing stratospheric O_3 concentrations) into the troposphere results in a enhanced OH production. Furthermore, the tropical and global variability of τ_{CH4} in S4 is correlated with the MG II solar cycle, which is a dimensionless measure of the mid-ultraviolet solar activity and a composite of UV irradiances of several satellite instruments [*DeLand and Cebula*, 1993] (see also ftp://ftp.ngdc.noaa.gov/STP/SOLARDATA/SOLARUV/UVCOMPOSITE). The solar cycle substantially affects the interdecadal stratospheric O_3 variability in the tropics. The correlation coefficients are about r = 0.75 as shown in Figure 5. However, especially in the SH high latitudes the lifetime signal is more dependent on stratospheric ozone depletion, although the influence on global OH and methane lifetime is limited. Simulation S5 shows that the combined trends of all precursor gases increases the lifetime of CH_4 by 0.12% yr^{-1} and therefore decreases OH. S6 and S7 show that both CO and CH_4 changes can strongly increase the methane lifetime by 0.21 ± 0.01 and 0.13 ± 0.01% yr^{-1}, respectively and thus negatively affect the OH concentrations. Also NMVOC emission changes have a negative effect on OH (-0.15% yr^{-1}). In contrast the changes in NO_x emissions have a strong positive effect on OH (S8) that globally amounts to 0.41% yr^{-1}.

[36] Simulation S6 shows a smooth increasing CH_4 lifetime, which can be attributed to the negative feedback effect of increasing methane concentrations on OH and its own lifetime. This feed-back is defined by feed-back factor s in equation 8:

$$s = \frac{\delta ln \tau}{\delta ln[CH_4]} \tag{8}$$

The feed-back factor of s = 0.26, calculated for simulation S6, is consistent with the feedback factors (0.25–0.31) presented by *Prather et al.* [2001, Table 3].

[37] Almost all interannual variability in the calculated lifetimes results from the stratospheric ozone boundary conditions and not from a variation of the surface emissions (Table 3). This is expected since the interannual variations of the surface emissions were rather small (Figure 1). This result would probably have been different, if we would have included variability of, for example, biomass burning emissions, which are dependent on, e.g., the meteorological conditions.

3.5. Principal Component Analysis of Spatial Patterns

[38] The large-scale meteorological processes that underlie the variability in ozone, humidity and photolysis rate

Table 5. Correlation r of τ_{CH4} of Simulation S2 With OH Loss Rates L_{OH}, Primary Production P_{OH}, Water Vapor H_2O, Primary Production Normalized for O_3 (P_{OH}/O_3), and Primary Production Normalized for H_2O (P_{OH}/H_2O)

Parameter	90N–45N	45N–EQ	EQ–45S	45S–90S	Global
L_{OH}	0.32	0.70	−0.25	0.06	0.19
P_{OH}	−0.96	−0.91	−0.96	−0.86	−0.96
H_2O	−0.86	−0.75	−0.87	−0.28	−0.85
P_{OH}/O_3	−0.95	−0.94	−0.43	−0.36	−0.76
P_{OH}/H_2O	−0.69	−0.14	0.20	−0.44	0.07

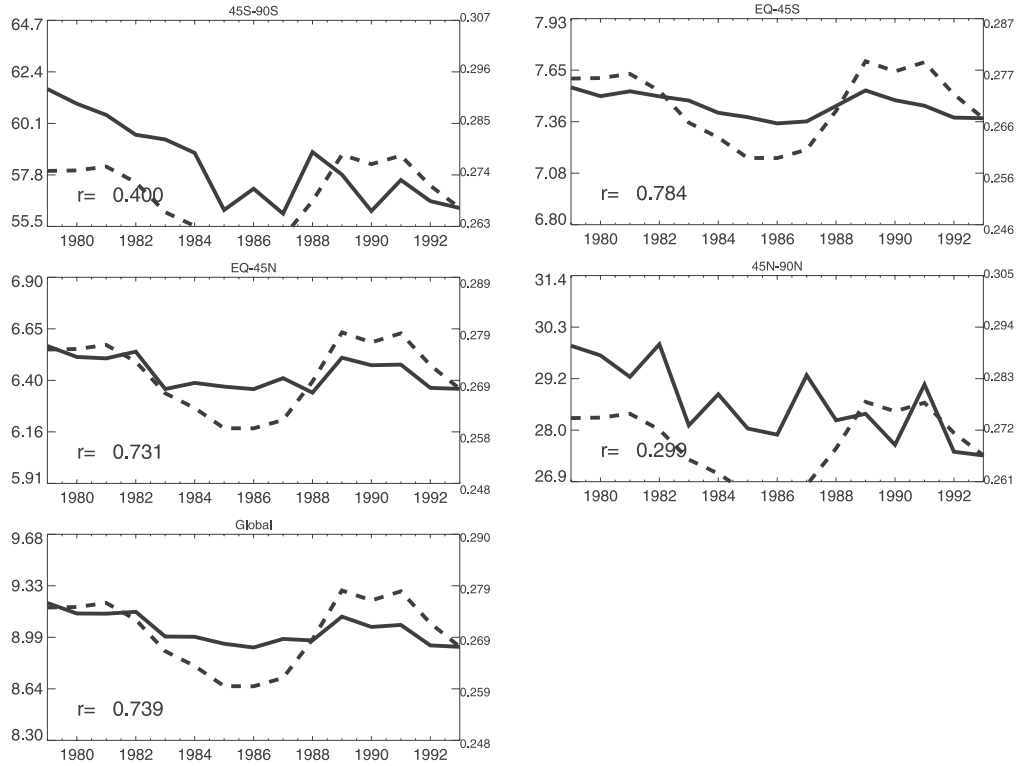

Figure 5. Correlation of the lifetimes [years] calculated in simulation S4 and the solar cycle 11 (dashed line). Dimensionless solar cycle index values are on the right axis. We show four regional compartments and the global mean of the lifetime.

variations have been studied with a principal component (EOF) analysis applied to the tropical regions, where P_{OH} and OH concentrations maximize. The method is similar to that used by *Peters et al.* [2001]. In the tropics (19S–19N) a large part of the moisture variation can be explained by ENSO, since EOF-analysis of the spatial patterns of monthly moisture fields shows that about 27% (r = 0.57) of the variance can be explained by the first principal component. Interannual tropospheric ozone variations are also dominated by ENSO (25%, r = 0.6) [*Peters et al.*, 2001]. Photolysis rates, being sensitive to stratospheric ozone abundance, vary primarily with the Quasi-Biennial Oscillation (QBO), and with the solar cycle as shown above. The resulting spatial and temporal distributions of the OH and τ_{CH4} fields in simulation S1, however, could not be related to these large-scale processes (only 8% of spatial-temporal variation could be explained by an ENSO signal). The most likely explanation is that the variance is averaged out in the large spatial regions and annual timescale analysis considered in our analysis. Further, ENSO has opposing effects of water vapor and ozone variations, which diminish its effect on CH_4 lifetime and OH.

4. Discussion and Conclusions

[39] Current knowledge on temporal and spatial changes in global emissions, stratospheric ozone and interannual variability in meteorology was brought together in a validated global chemistry-transport model. We calculated the trend and variability of the methane lifetime as a measure for the global OH concentration in the 1979–1993 time frame. From a systematic analysis we could untangle the various causes of the trend and variability in OH in this period.

[40] Over 1979–1993 we find a significant increase in global OH, which weighted by methane, amounts to 0.24 ± 0.06% yr^{-1} for the period 1979–1993. The uncertainty is the 1 σ standard deviation of the trend analysis. The actual uncertainty in the trend will also depend on the accuracy of the model representation of processes as well as on processes which are not included in the model. Given the large interannual variability of OH (globally 1.5%), the analysis period of 15 years is still rather short for a robust trend analysis.

[41] Our trend results can be compared with the work of *Krol et al.* [1998, 2001], who calculated a positive OH trend (weighted to MCF) of 0.46 ± 0.6% yr^{-1} for the period 1978–1993. The uncertainty range in their analysis reflects the uncertainty of the OH calculations using a limited set of observations and uncertain emissions of methyl chloroform. In contrast, the errors in our calculated global methane lifetime reflects the standard deviation of the trend analysis.

[42] In a recent study, *Prinn et al.* [2001] derive a positive OH trend of 1.4% yr^{-1} for the period 1979–1989. We calculate for the same period 1979–1989 a significantly smaller OH trend of +0.28% ± 0.09 yr^{-1}. It is important to mention here that a recent study [*Dentener et al.*, 2003] showed that the calculated OH trend of S1 was consistent with observed methane growth rates and an estimate of the growth of methane emissions of 2.7 Tg CH_4 yr^{-1}. In contrast the much larger OH trend in the 1979–1989 period as inferred from MCF measurements by *Prinn et al.* [2001] would require much larger CH_4 emission increases to be

consistent with methane observations. CH_4 emissions would have to additionally increase by about 6 Tg yr $^{-1}$, if the estimate of 1.4% yr^{-1} OH trend for the period 1979–1989 were realistic. This would imply that during this period CH_4 emissions would have been increasing by an rate of (6 + 2.7 =) 8.7 Tg yr^{-1}. We think such an annual increase is unlikely for the anthropogenic CH_4 [*van Aardenne et al.*, 2001] as well as the natural emissions. The latter is unlikely since the tropical temperature trends, which could influence, e.g., wetland emissions, were smaller than 0.02 K yr^{-1} over the period 1979–1993. However, as suggested by *Dentener et al.* [2003] the interannual variability of temperatures could indeed have influenced methane emissions. Other model studies were presented by *Karlsdòttir and Isaksen* [2000] and *Karlsdòttir et al.* [2000]. They found a global mean OH increase of 0.43% yr^{-1} over the period 1980–1996 (and an increase of 0.4% yr^{-1} over period 1980–1993). This increase is only due to emission changes in the ozone precursor gases (CO, NO_x and NMVOCs) and increases in CH_4 concentrations because the model calculations were performed with one fixed year of GCM climatology. Their estimates can best be compared with our simulation S5 which, however, gives a small negative trend in OH of −0.12% yr^{-1}. One explanation for the difference in the calculated OH trend could be the high sensitivity of the methane lifetime to regional changes in especially the CO and NO_x emission distributions [*Gupta et al.*, 1998; *Karlsdòttir et al.*, 2000]. Therefore we compared the respective emission estimates and trends, which appear to be rather similar globally. Regionally, the main difference is the somewhat smaller CO emission reductions in North America and Europe in our model, and the slightly larger NO_x increases of 1 Tg N integrated for the period 1980–1993 in high-emission regions in S.E. Asia, China and India. It is therefore difficult to pinpoint the difference in our model results to emissions alone, or perhaps to other model differences, such as the model resolution, specific year of meteorology and model boundary conditions. However, if we ignore the effect of increasing CH_4 concentrations by comparing S6 and S5, we also find a positive trend in OH of about 0.10% yr^{-1}. Improved emission inventories and their spatial-temporal development remain imperative to reliably simulate oxidant trends.

[43] Our sensitivity studies show that meteorological variability (S2) and the changes of stratospheric ozone concentrations (S4) have a stronger influence on the variability and trend of the CH_4 lifetime than the changes in the precursor emissions (S5) (Table 3).

[44] The results of S4 are consistent with those of *Bekki et al.* [1994], who calculated a global OH trend of 0.2–0.3% yr^{-1} between 1979 and 1990 due to the effect of decreasing stratospheric ozone concentrations. In simulation S4 we also show that in the tropics the methane lifetime of S4 had a clear correlation with the 11 year solar cycle. A solar minimum reduces stratospheric ozone production and leads to a minimum of stratospheric ozone in the tropics. As a consequence the global methane lifetime is reduced by about 0.2 years due to the higher UV actinic fluxes reaching the troposphere, and hence higher primary production P_{OH}.

[45] Methane lifetimes are strongly influenced by meteorology. Table 3 shows that most of the calculated trend and much of the variability in S1 could be explained by simulation S2. Meteorology can influence OH in many ways. There are differences in modeled large-scale transport and convection, which substantially influence the concentration fields of photo-oxidant precursor gases such as NO_x and CO. Further, in our model NO_x produced by lightning is dependent on meteorology since it is coupled to the subgrid-scale convection. This results in an interannual variability of 0.5 Tg yr^{-1} (about 10% of the global lightning NO_x source and about 1.5% of the total NO_x emissions). Meteorology also influences the influx of stratospheric ozone into the troposphere, as well as the thickness of the stratospheric ozone layer and hence the UV flux penetrating into the troposphere. The influence of stratospheric ozone influx into the troposphere on τ_{CH4} was evaluated to be relatively weak. However, in simulation S2 the lifetime of CH_4 is highly correlated with the primary production of OH resulting in a global correlation coefficient of r = −0.96. Most of the correlation could be attributed to the variable influence of water vapor, and less to the influence of UV actinic flux into the troposphere. In the tropics (19N–19S) humidity and ENSO are strongly correlated; also tropospheric ozone and ENSO are (less strongly) correlated [*Peters et al.*, 2001]. However, no strong correlation was found between the spatial and temporal patterns of τ_{CH4} and ENSO in the tropical regions. We expect that the influence of moisture on OH and τ_{CH4} involves a complex cascade of feed-backs that obscure the signature of ENSO on the finer regional and temporal scales, which needs further study.

[46] Although the ECMWF-ERA15 (1979–1993) is a state-of-the-art meteorological reanalysis there are considerable uncertainties about almost all aspects of the hydrological cycle and especially in the tropics where very few measurements are available to constrain the reanalysis model. *Stendel and Arpe* [1997] mention a slightly decreasing trend of evapotranspiration, which "tends to dry the atmosphere". Our analysis does not confirm this. The troposphere seems during the 2nd half of the ERA15 period somewhat more humid than the 1st half and there are large regional differences between ENSO and non-ENSO years. *Slingo et al.* [2000] compare water vapor variability in ECMWF-ERA15, which used a 1-DVar assimilation of satellite and sonde water vapor, and the Hadley centre climate model, which was only constrained by observed seawater surface temperatures (SST). Global average column water vapor showed a similar response to SST in both models, although the variability and feedback in ERA15 was larger than in the Hadley model. *Johnson et al.* [2002] used output from the HadCM3 climate model in the off-line transport-chemistry model STOCHEM and found a calculated standard deviation of methane concentrations of 1.4 ppbv yr^{-1}, which corresponds to a variability of methane lifetime of 0.64%. In our simulation S2 we found a calculated variability in methane lifetimes of 1.6% consistent with the higher moisture variability in ECMWF-ERA15 than in HadCM3.

[47] Given this conflicting information, and the importance and uncertainties associated with water vapor, we recommend that the calculated trends due to meteorology should be considered with some care. We nevertheless emphasize that the ECMWF ERA15 reanalysis that we have used for our assessment provides the most accurate

and consistent and systematic information currently available on meteorological trends in the period 1979–1993. The important role of humidity on OH has been identified before, for example, by *Stevenson et al.* [2000], who found that the change of OH in future climate simulations was strongly influenced by climate change and "in particular higher absolute humidity".

[48] An important issue for future work will be to include interannual variations of emissions of trace gases that vary with the meteorology. NO_x emissions from soils, CH_4 from wetlands, CO, CH_4, NMVOC, and NO_x from biomass burning depend on meteorology and hence can influence OH and methane lifetimes. For instance natural methane emissions variability of 8 Tg CH_4 yr^{-1} was estimated from mass balance by *Dentener et al.* [2003] using a combination of a-priori emissions, and nudging of model CH_4 to observations. In that work, however, we assumed the calculated OH fields to be perfect. Although it is likely that such methane emission variability is realistic, we could theoretically also have explained the model results by assuming an additional variability of OH. Assuming an OH-methane feedback factor of 0.26 [*Prather et al.*, 2001], the global OH variability, corresponding to a methane burden variation of 8 Tg CH_4 yr^{-1}, would amount to about 0.05% yr^{-1}. Thus under this assumption the standard deviation of the trend of simulation S1 of would be 0.11% yr^{-1} rather than 0.06% yr^{-1}.

[49] New estimates of global anthropogenic emission trends for the period 1970–1995 have very recently become available (J. Olivier, personal communication, 2002), and should be included in future work. Recent work by *Parrish et al.* [2002] casts doubt on the accuracy of the current generation of emission inventories, since CO measurement in a number of USA cities indicate larger decreases of CO emissions than currently reported by emission inventories. ECMWF is currently performing a new reanalysis of the period 1957–2001 (see www.ecmwf.int/research/era), which will yield important additional information.

[50] We summarize the conclusions as follows.

[51] 1. This work gives a consistent picture of all factors that control the trend and variability of OH (see Figure 6). These first results indicate that OH has been relatively stable during the period 1979–1993. Previous reports [*Prinn et al.*, 2001] on strong OH changes in the 1980s and 1990s are not supported by our calculations nor are they consistent with our knowledge of the methane cycle [*Dentener et al.*, 2003].

[52] 2. Meteorological variability has an important influence on OH variability and also explains a large part of the computed trend. Water vapor trends and variability play an important but uncertain role in the meteorology induced OH trends.

[53] 3. Variability and trends of stratospheric ozone are important drivers of OH interannual changes. Trends induced by surface emissions of all ozone precursor gases have the net effect to decrease OH, with CH_4, CO and NMVOC having a relatively large negative influence on OH and NO_x a strong positive effect (Figure 6). Stratospheric ozone loss leads to a net increase of OH. The combined OH changes of these effects in the period 1979–1993 are small. The ratio of NO_x and CO emissions may be critical in determining OH trends [*Wang and Jacob*, 1998; *Lelieveld et al.*, 2002].

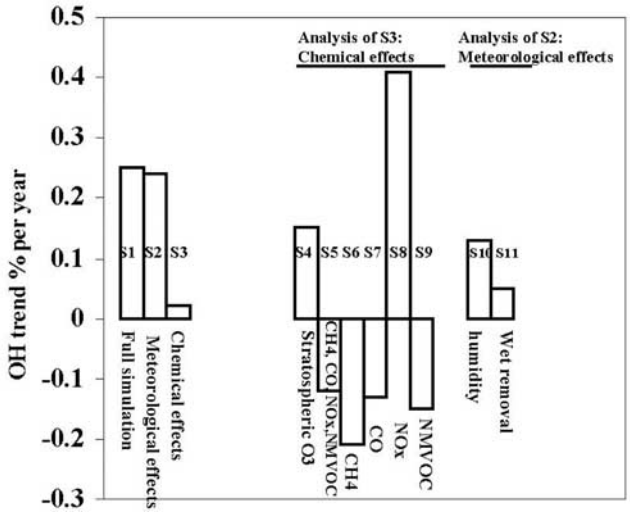

Figure 6. Summary of global trends [% yr^{-1}] calculated for all simulations. For description of simulations, see Table 2. Note that nonlinear effects are present in the simulations.

[54] 4. The computed OH variability as inferred in this study may be underestimated since we did not take into account variability of NO_x and other emissions by biomass burning and soils. This will be an important topic for future studies.

[55] **Acknowledgments.** We thank Sigrun Karlsdòttir for her help in discussing the differences in emissions between our studies. MvW acknowledges financial assistance within the EU-project UTOPIHAN-ACT (EVK-CT2001-00099). We appreciate the critical but constructive comments of the two anonymous reviewers.

References

Bekki, S., K. S. Law, and J. A. Pyle, Effect of ozone depletion on atmospheric CH_4 and CO concentrations, *Nature*, *371*, 595–597, 1994.

Berntsen, T., I. Isaksen, G. Myhre, J. S. Fuglestvedt, F. Stordal, T. A. L., R. S. Freckleton, and K. Shine, Effects of anthropogenic emissions on tropospheric ozone and its radiative forcing, *J. Geophys. Res.*, *102*, 28,101–28,126, 1997.

DeLand, M. T., and R. P. Cebula, Composite Mg II solar activity index for solar cycles 21 and 22, *J. Geophys. Res.*, *98*, 12,809–12,823, 1993.

Dentener, F. J., J. Feichter, and A. Jeuken, Simulation of the transport of ^{222}Rn using on-line and off-line global models at different horizontal resolutions: A detailed comparison with measurements, *Tellus, Ser. B*, *51*, 573–602, 1999.

Dentener, F. J., M. van Weele, M. Krol, S. Houweling, and P. van Velthoven, Trends and inter-annual variability of methane emissions derived from 1979–1993 global CTM simulations, *Atmos. Chem. Phys.*, *3*, 73–88, 2003.

Derwent, R., The influence of human activities on the distribution of hydroxyl radicals in the troposphere, *Philos. Trans. Math. Phys. Eng. Sci.*, *354*, 501–531, 1996.

Dlugokencky, E. J., K. A. Masarie, P. M. Lang, and P. P. Tans, Continuing decline in the growth rate of the atmospheric methane burden, *Nature*, *393*, 447–450, 1998.

Fortuin, J. P. F., and H. Kelder, An ozone climatology based on ozonesonde and satellite measurements, *J. Geophys. Res.*, *103*, 31,709–31,734, 1998.

Gibson, R., P. Kallberg, and S. Uppsala, The ECMWF re-analysis (ERA) project, *ECMWF Newsl. 73*, Eur. Cent. for Medium-Range Weather Forecasts, Reading, U. K., 1997.

Gupta, M., R. J. Cicerone, and S. Elliot, Perturbation to global tropospheric oxidizing capacity due to latitudinal redistribution of surface sources of NO_x, CH_4, and CO, *Geophys. Res. Lett.*, *21*, 3931–3934, 1998.

Houweling, S., F. J. Dentener, and J. Lelieveld, The impact of nonmethane hydrocarbon compounds on tropospheric photochemistry, *J. Geophys. Res.*, *103*, 10,673–10,696, 1998.

Houweling, S., F. J. Dentener, J. Lelieveld, B. Walter, and E. J. Dlugokencky, The modeling of tropospheric methane: How well can point measure-

ments be reproduced by a global model?, *J. Geophys. Res.*, *105*, 8981–9002, 2000.

Johnson, C., D. Stevenson, W. Collins, and R. Derwent, Interannual variability in methane growth rate simulated with a coupled ocean-atmosphere-chemistry model, *Geophys. Res. Lett.*, *29*(19), 1903, doi:10.1029/2002GL015269, 2002.

Karlsdòttir, S., and I. S. A. Isaksen, Changing methane lifetime: Possible cause for reduced growth, *Geophys. Res. Lett.*, *27*, 93–96, 2000.

Karlsdòttir, S., I. S. A. Isaksen, G. Myhre, and T. K. Berntsen, Trend analysis of O_3 and CO in the period 1980–1996: A three-dimensional model study, *J. Geophys. Res.*, *105*, 28,907–28,933, 2000.

Krol, M., and J. Lelieveld, Can the variability in tropospheric OH be deduced from measurements of 1,1,1-trichloroethane (methyl chloroform)?, *J. Geophys. Res.*, *108*(D3), 4125, doi:10.1029/2002JD002423, 2003.

Krol, M., and M. Van Weele, Implications of variation of photodissociation rates for global atmospheric chemistry, *Atmos. Environ.*, *31*, 1257–1273, 1997.

Krol, M., P. J. van Leeuwen, and J. Lelieveld, Global OH trend inferred from methylchloroform measurements, *J. Geophys. Res.*, *103*, 10,697–10,711, 1998.

Krol, M., P. J. Van Leeuwen, and J. Lelieveld, Reply to comment by R. G. Prinn and J. Huang on "Global OH trend inferred from methylchloroform measurements", *J. Geophys. Res.*, *106*, 23,159–23,164, 2001.

Krol, M., J. Lelieveld, D. Oram, G. Sturrock, S. Penkett, C. Brenninkmeijer, V. Gros, J. Williams, and H. Scheeren, Continuing emissions of methyl chloroform from Europe, *Nature*, *421*, 131–135, 2003.

Landgraf, I., and P. J. Crutzen, An efficient method for online calculations of photolysis and heating rates, *J. Atmos. Sci.*, *55*, 863–878, 1998.

Lawrence, M. G., P. Joeckl, and R. von Kuhlman, What does the global mean OH concentration tell us?, *Atmos. Chem. Phys.*, *1*, 37–49, 2001.

Lelieveld, J., and F. J. Dentener, What controls tropospheric ozone?, *J. Geophys. Res.*, *105*, 3531–3551, 2000.

Lelieveld, J., W. Peters, F. J. Dentener, and M. C. Krol, Stability of tropospheric hydroxyl chemistry, *J. Geophys. Res.*, *107*(D23), 4715, doi:10.1029/2002JD002272, 2002.

Marland, G., T. A. Boden, and R. J. Andres, CO_2 emissions trends: A compendium of data on global change, technical report, Carbon Dioxide Anal. Cent., Oak Ridge Natl. Lab., Oak Ridge, Tenn., 2000.

Martinerie, P., G. Brasseur, and C. Granier, The chemical composition of ancient atmospheres, *J. Geophys. Res.*, *100*, 14,291–14,304, 1995.

McPeters, R. E. A., Nimbus-7 total ozone mapping spectrometer (TOMS) data products user's guide, *NASA Ref. Publ., 1384*, 1996.

Olivier, J. G. J., A. F. Bouwman, J. J. M. Berdowski, C. Veldt, J. P. J. Bloos, A. J. H. Visschedijk, C. W. M. van der Maas, and P. Y. J. Zandveld, Sectoral emission inventories of greenhouse gases for 1990 on a per country basis as well as on 1° × 1°, *Environ. Sci. Policy*, *2*, 241–263, 1999.

Parrish, D. D., M. Trainer, D. Hereid, E. J. Williams, K. J. Olszyna, R. A. Harley, J. F. Meagher, and F. C. Fehsenfeld, Decadal change in carbon monoxide to nitrogen oxide ratio in U.S. vehicular emissions, *J. Geophys. Res.*, *107*(D12), 4140, doi:10.1029/2001JD000720, 2002.

Peters, W., M. Krol, F. J. Dentener, and J. Lelieveld, Identification of an El Niño oscillation signal in a multiyear global simulation of tropospheric ozone, *J. Geophys. Res.*, *106*, 10,389–10,402, 2001.

Prather, M., et al., Atmospheric chemistry and greenhouse gases, in *Climate Change 2001, The Scientific Basis: Contribution of Working Group I to the Third assessment Report of the Intergovernmental Panel on Climate*, edited by J. T. Houghton et al., pp. 239–287, Cambridge Univ. Press, New York, 2001.

Prinn, R. G., and J. Huang, Comment on "Global OH trend inferred from methylchloroform measurements" by M. Krol et al., *J. Geophys. Res.*, *106*, 23,151–23,157, 2001.

Prinn, R. G., R. F. Weiss, B. R. Miller, J. Huang, F. N. Alyea, D. M. Cunnold, P. B. Fraser, D. E. Hartley, and P. G. Simmonds, Atmospheric trends and lifetime of CH_3CCl_3 and global average hydroxyl radical concentrations based on 1978–1994 ALE/GAGE measurements, *Science*, *269*, 187–192, 1995.

Prinn, R. G., et al., Evidence for substantial variations of atmospheric hydroxyl radicals in the past two decades, *Science*, *292*, 1882–1888, 2001.

Slingo, A., J. Pamment, R. Allan, and P. Wilson, Water vapor feedback in the ECMWF reanalysis and Hadley centre climate model, *J. Clim.*, *13*, 3080–3098, 2000.

Stendel, M., and K. Arpe, Evaluation of the hydrological cycle in reanalyses and observations, *ECMWF Reanal. Proj. Rep. Ser. 6*, Eur. Cent. for Medium-Range Weather Forecasts, Reading, U. K., 1997.

Stevenson, D. S., W. J. Johnson, W. J. Collins, R. G. Derwent, and J. M. Edwards, Future tropospheric ozone radiative forcing and methane turnover- the impact of climate change, *Geophys. Res. Lett.*, *27*, 2073–2076, 2000.

van Aardenne, J. A., F. J. Dentener, J. G. J. Olivier, C. G. M. Klein Goldewijk, and J. Lelieveld, A 1° × 1° resolution data set of historical anthropogenic trace gas emissions for the period 1890–1990, *Global Biogeochem. Cycles*, *15*, 909–928, 2001.

Wang, Y., and D. J. Jacob, Anthropogenic forcing on tropospheric O_3 and OH since preindustrial times, *J. Geophys. Res.*, *103*, 31,123–31,135, 1998.

Ziemke, J., and S. Chandra, Seasonal and interannual variabilities in tropical tropospheric ozone, *J. Geophys. Res.*, *104*, 21,425–21,442, 1999.

P. Bergamaschi and F. Dentener, JRC, Institute for Environment and Sustainability, I-21020 Ispra, Italy. (peter.bergamaschi@jrc.it; frank.dentener@jrc.it)

M. Krol and W. Peters, IMAU, Utrecht University, Princetonplein 5, NL-3584 CC Utrecht, Netherlands. (krol@phys.uu.nl; peters@phys.uu.nl)

J. Lelieveld, MPI for Chemistry, PB 3060, D-55020 Mainz, Germany. (lelieveld@mpch-mainz.mpg.de)

M. van Weele, Department of Applied Physics, Eindhoven University of Technology, 5600 MB Eindhoven, Netherlands. (weelevm@knmi.nl)